International Journal of Technology 13(8) 1796-1805 (2022)
Received June 2022 / Revised November 2022 / Accepted December 2022

International Journal of Technology

http://ijtech.eng.ui.ac.id

The Study of Methylene Blue Loading into Chitosan-graft-Maleic Sponges

Daniel Timotius[1], Yuni Kusumastuti[2*], Rozita Omar[3], Razif Harun[3], Siti Mazlina Mustapa Kamal[4], Siti Nurul Aisyiyah Jenie[5], Himawan Tri Bayu Murti Petrus[2]

[1]*Department of Chemical Engineering, Faculty of Industrial Engineering, Universitas Pembangunan Nasional "Veteran" Yogyakarta, Jl. SWK 104, Yogyakarta 55283, Indonesia*
[2]*Department of Chemical Engineering, Faculty of Engineering, Universitas Gadjah Mada, Jalan Grafika 2, Yogyakarta 55281, Indonesia*
[3]*Department of Chemical and Environmental Engineering, Faculty of Engineering, Universiti Putra Malaysia, Serdang 43400, Selangor, Malaysia*
[4]*Department of Food and Process Engineering, Faculty of Engineering, Universiti Putra Malaysia, Serdang 43400, Selangor, Malaysia*
[5]*Research Centre for Chemistry, National Research and Innovation Agency (BRIN), Kawasan Puspiptek Building 452, Serpong, Tangerang Selatan 15314, Indonesia*

Abstract. This work succeeded in synthesizing sponges from chitosan-graft-maleic anhydride. Chitosan and maleic anhydride at a certain mass ratio (1:2, 1:1; and 2:1) were reacted in dimethyl sulfoxide (DMSO) at 60°C for 24 hours. While the gel formation was carried out in distilled water using a dialysis tube. The removal of DMSO from the gel was carried out by soaking the gel in distilled water for two days. After that, the obtained gel was frozen at -25°C overnight before being lyophilized under a vacuum at -40°C for 24 hours. The dry sponge weight obtained after lyophilization is about 5.61% – 6.77% (dry sponge/wet gel). FTIR and TG/DTA then characterized the sponges. The intensity of the new strong FTIR band appeared in the chitosan-graft-maleic sponge at 1560.13 $cm^{-1,}$ which corresponds to the C=C strain. The results of TG/DTA showed that pure chitosan and sponge chitosan-maleate underwent two stages of degradation, namely evaporation of water and pyrolysis of organic compounds. The shift in the peak rate of degradation in the second stage occurred at 300°C for pure chitosan and at 340°C for a graft-chitosan-maleate sponge. Both results indicate that the reaction was successful. The drug loading capability was investigated using methylene blue as the drug model. The drug loading kinetics corresponded to a pseudo-first-order model with k_f ranging from 0.287 to 0.317 day^{-1}. According to the Freundlich model, the adsorption equilibrium with K_f and 1/n values was 4.923 mg/gram and 2.192, respectively.

Keywords: Chitosan, Drug delivery system, Maleic anhydride, Methylene blue, Sponges

1. Introduction

Sponges are porous materials synthesized from various materials and methods (Deb et al, 2018). It has many advantages in the field of biomaterials, such as wound dressings (Horio et al., 2010), tissue engineering (Nikolova & Chavali, 2019), and drug delivery systems (Cai et al., 2018). A large surface area is required to attach the active molecule or

*Corresponding author's email: yuni_kusumastuti@ugm.ac.id, Tel.: 0274-555320
doi: 10.14716/ijtech.v13i8.6133

drug in drug delivery systems. Not only surface area but also materials for drug delivery systems require several properties, such as non-toxicity, biocompatibility, and biodegradability (Patel et al., 2018). These properties are found in many natural polymers, one of which is chitosan (Peers et al., 2020).

Chitosan (1-4)-2-amino-2-deoxy-β-D-glucan is the second most abundant polysaccharide (Ali & Ahmed, 2018). And it is usually synthesized from the deacetylation of chitin (Sinha et al., 2004) which extracted from the exoskeleton of crustaceans (Liu et al., 2016). Chitosan and chitin can be distinguished by deacetylation (DD) degree. If the DD greater than 50%, it will consider as chitosan (Knidri et al., 2018). Chitosan has been extensively used as a drug delivery system due to its properties, namely non-toxic, biodegradable, and mucoadhesive (Krisanti et al., 2020). Chitosan has two active functional groups, amine and hydroxyl, and is usually further modified by other chemicals. Sponges from chitosan are made by lyophilization of gel or chitosan solution. Lyophilization or freeze-drying is a process in which water is frozen and removed through sublimation (primary drying) and desorption (secondary drying). In sponges, pore size is an important parameter (Deb et al., 2018). The pore size of the sponge can be controlled by varying several parameters, such as the geometry of the thermal gradient during freezing, ice crystal size, freezing temperature, and freezing rate (Pottathara et al., 2021).

Chitosan is usually reacted with a crosslinking agent to form a gel. There are many crosslinking agents with different interactions, namely chemical and physical crosslinkers (Hamedi et al., 2018). Chemical crosslinks are formed by irreversible covalent bonds between polymers and crosslinkers (Liu et al., 2014), whereas physical crosslinks are reversible interactions between polymers and crosslinkers (Croisier & Jérôme, 2013). In physical crosslinking, crosslinking can be found in the form of ions or ionic molecules. Chitosan is polycationic with a protonated amine group. Therefore, to physically crosslink chitosan, anions or anionic molecules are needed (Kono et al., 2013). Maleic anhydride becomes an attractive anionic molecule to use if it is to be further modified. Chitosan reacts with maleic anhydride through the amidation and esterification processes. After the reaction, chitosan has a cationic functional group from the protonated amine group and anionic functional group from the deprotonated carboxyl group, therefore it becomes a polyampholyte (Timotius et al., 2022).

The drug model used in this study is methylene blue. Methylene blue has a long journey as a drug that is applied on malaria diseases (Ashley & Phyo, 2018). Now, this cationic drug has been widely used, not only on malaria, but also on other diseases, namely methemoglobinemia, ifosfamide-induced neurotoxicity, paraplegic adrenaline-resistant shock, and Alzheimer's (Schirmer et al., 2011). Another study uses methylene blue to enhance the apoptosis of cells in lung cancer by photodynamic therapy (Lim et al, 2013). Another study reviews its potency as anti-aging drug (Xue et al., 2021).

This study is aiming the potency of chitosan-graft-maleic sponges as a drug carrier. In this study, the lyophilization method successfully synthesized a novel chitosan base sponge from chitosan and maleic anhydride. The modified chitosan solution is prepared by reacting low molecular weight chitosan with maleic anhydride in dimethyl sulfoxide (DMSO). Furthermore, the gel formation is carried out by dialysis of the modified chitosan solution under aquadest. Then before lyophilization, the gels were frozen at –25°C. The obtained sponges are then further characterized.

2. Methods

2.1. Materials

Low molecular weight chitosan (50 – 190 kDa, 75 – 85% DD) was obtained from Sigma Aldrich, USA. Acetic acid (100%) was supplied from Merck, Germany. Maleic anhydride (>99% purity) was purchased from Nacalai Tesque Inc., Japan. Methylene blue was obtained from Merck, India. Merck, Japan, supplied dimethyl sulfoxide (DMSO). All reagents were used without further purification or treatment.

2.2. Methods

2.1.1. Synthesis of Chitosan-graft-Maleic Sponges

The chitosan-graft-maleic (Chi-MA) synthesis followed previous studies with slight modifications (Zhou et al., 2017). The scheme of sponges synthesis is provided in Figure 1. About 1 gram of chitosan is dissolved in 50 mL of dimethyl sulfoxide. After the chitosan was dissolved entirely, maleic anhydride was added to the solution, followed by stirring at 300 rpm, 60°C for 24 hours. Gel formation was carried out using a dialysis tube. After the reaction, the solution is placed in cellulose dialysis tubing (MWCO 15 kDa) and dialyzed under deionized water to form a gel. The removal of DMSO from the gel was carried out by soaking the gel in distilled water for two days. Afterward, the obtained gel was frozen at -25°C overnight before being lyophilized under a vacuum at -40°C for 24 hours. This method was performed for several MA masses (0.5 grams, 1 gram, and 2 grams) labeled Chi-MA-21, Chi-MA-22, and Chi-MA-24.

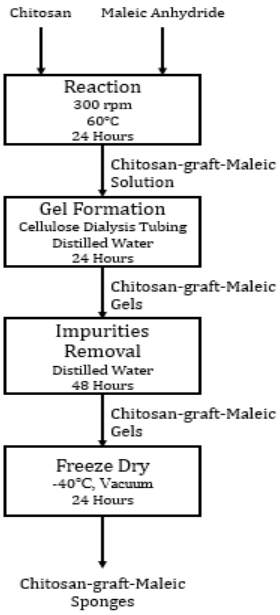

Figure 1 Preparation of Chitosan-graft-Maleic Sponges

2.1.2. Characterization

FTIR and thermogravimetric analysis were carried out for the characterization of chitosan sponges. The FTIR study was performed by SHIMADZU IR Pestige-21. The sponges were scanned with wavenumber ranging from 400 – 4000 cm-1. The thermogravimetric analysis (TGA) study was conducted by NEXTA STA (Hitachi STA200RV) with actual view sample observations, and 15 mg of the sample was heated to a temperature of 900°C with a heating rate of 10°C /min.

2.1.3. Drug Loading

Drug loading was carried out using the Chi-MA gel state. Methylene blue was dissolved in deionized water and analyzed using a Vis Spectrophotometer (Genesys 20) as the initial

concentration (C_o). Chi-MA gel was weighed and immersed in methylene blue solution. A decrease in concentration (C_t) was observed for several increments. Observations are completed when equilibrium has been reached. The adsorbed methylene blue (q_t) was calculated using Equation 1, where the V and m_D are the volumes of the methylene blue solution and the dry sponge.

$$q_t = \frac{(C_o - C_t)}{m_D} \times V \quad (1)$$

Kinetic studies were evaluated using two simple models, namely pseudo-first-order (PFO, Equation 2) and pseudo-second-order (PSO, Equation 3) (Syafiuddin et al., 2018). Where q_e, k_f, and k_s are the drug absorbed at equilibrium, PFO constant, and PSO constant, respectively. Fitting data minimizes the sum of square error (SSE) as described in Equation 4.

$$q_t = q_e\left(1 - \exp\left(-k_f t\right)\right) \quad (2)$$

$$q_t = \frac{k_s\, q_e^2\, t}{1 + k_s q_e t} \quad (3)$$

$$SSE = \left(q_{t,exp} - q_{t,calc}\right)^2 \quad (4)$$

The adsorption model evaluation was conducted by two different models: Langmuir adsorption isotherm and Freundlich adsorption isotherm. The Langmuir model was presented using Equation 5, while the Freundlich model was shown in Equation 6 (Ayawei et al., 2017). The adsorption isotherm was conducted by measuring the equilibrium state of drug loading.

$$q_e = \frac{k_L\, C_e\, q_m}{1 + k_L C_e} \quad (5)$$

$$q_e = K_f (C_e)^{1/n} \quad (6)$$

3. Results and Discussion

3.1. Gel Preparation

The gel synthesis is successfully obtained up to 2:1 of MA to chitosan mass ratio. According to previous work (Zhou et al., 2017), the MA to chitosan ratio of about 3.5:1 makes the modified chitosan dissolve in the water instead of gel formation. It might happen because most of the amine groups are grafted by MA. Therefore, carboxyl groups instead of amine groups will dominate the chitosan. In the present work, 2:1 is being a maximum MA to chitosan ratio. The appearance of the gel is presented in Figure 1.

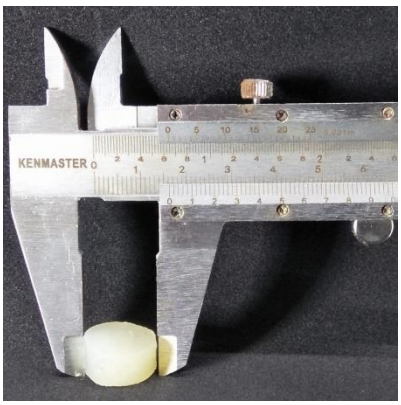

Figure 2 Gel State of Chitosan-graft-Maleic

The drying process of the gel is performed with two different methods, namely oven and freeze-drying. The oven-drying process shows an extreme shrinkage in the gel volume,

as shown in Figure 2a. This might have happened because the polymers cannot hold their structure. Unlike the oven-drying process, the freeze-drying or lyophilization process creates a sponge with low shrinkage, and the polymer can maintain its structure, as presented in Figure 2b. The shrinkage on oven drying is about 92.97% in volume, while freeze-dried sponge only shrank about 12.11%. This is occurred due to the sublimation process when the ice crystal is directly converted into a gas state (Kassem et al., 2015). The sponge's sample varies from 5.61 – 6.77%, while the rest is water.

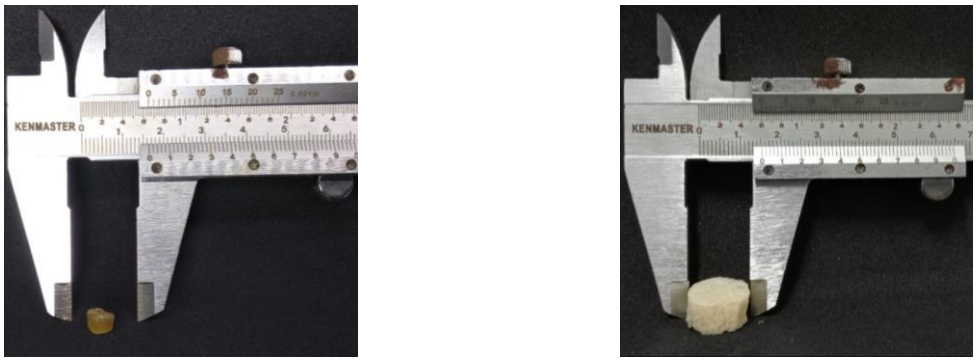

(a) (b)

Figure 3 Result of Oven Drying (a) and Freeze Drying (b) of Chi-MA Gels

3.2. Component Analysis

FTIR study on chitosan and Chi-MA-24 is conducted to observe each sample's functional group. Both results are shown in Figure 3. The FTIR spectrum of pure chitosan shows a broad peak at around 3443.28 cm^{-1}, which corresponds to the hydrogen bond of –NH and –OH stretching (Barleany et al., 2020). Amide I (C=O) and amide II (C–N) groups around 1658.80 and 1558.48 cm^{-1} (Kusumastuti et al., 2017; Haerudin et al., 2010) respectively, it appears due to the incomplete deacetylation of chitosan. The C–O–C stretching vibration appears at 1075.12 cm^{-1}, while the C–N stretches around 1311.35 cm^{-1} (Timotius et al., 2022). The result of Chi-MA-24 FTIR spectra shows a strong intensity at 1560.13 cm^{-1} , which corresponds to the presence of C=C stretching of grafted maleic anhydride (Lavanya et al., 2017). A sharper peak at 3443.28 cm^{-1} corresponds to the appearance of a hydrogen bond from the COOH functional group introduced on the chitosan backbone. It confirms the introduction of maleic on the chitosan backbone (Lavanya et al., 2017).

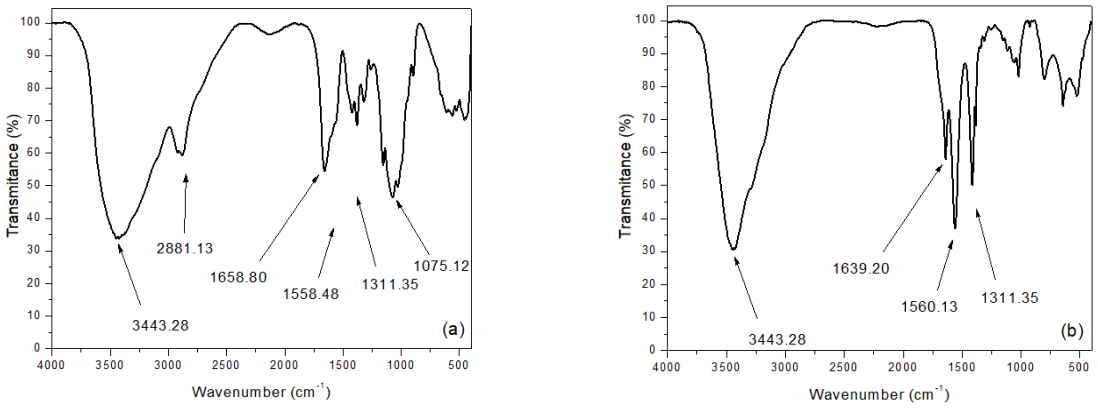

Figure 4 FTIR Spectra of Pure Chitosan (a) and Chitosan-graft-Maleic (b)

3.3. Thermogravimetric Analysis

The study is conducted to analyze the thermal stability of the Chi-MA samples. The result of TG/DTA from Chi and Chi-MA samples is presented in Figure 5. The result shows

that the first endothermic peak in DTA result at 82.56°C for pure chitosan and around 63-67°C for Chi-MA are due to the evaporation of water and volatile organic compound (Kusumastuti et al., 2020), which in line with the TG result. At the same time, the second endothermic flow corresponds to the glass transition temperature. The rate of degradation of chitosan and Chi-MA samples consists of 2 steps, as shown in Figure 5b. The first step is due to the samples' drying process, water evaporation, and volatile organic matter. In contrast, the second step occurs due to the degradation of organic compounds to form char. In the first step of pure chitosan, water evaporation occurs up to 100°C with a weight loss of about 15%. Meanwhile, the primary degradation occurs from about 250 to 450°C, with a minimal degradation rate. It is consistent with another study (Kumar & Koh, 2012). The degradation pattern of Chi-MA samples is similar to pure chitosan. However, there is a slight shift in the degradation rate between chitosan and Chi-MA samples, as shown in Figure 5a. The chitosan has a steeper degradation rate, while the Chi-MA samples are thermally more stable.

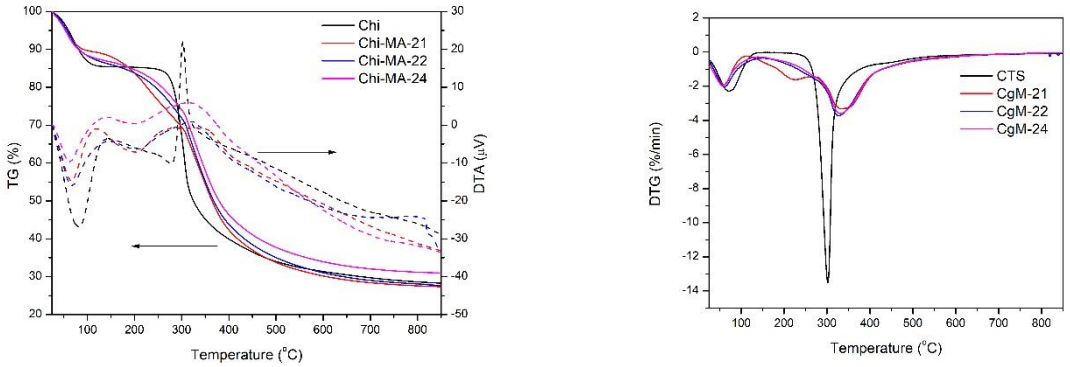

(a) (b)

Figure 5 TG/DTA of Chi and Chi-MA Samples at 10°C/min Heating Rate

3.4. Drug Loading

The result of methylene blue adsorption into the hydrogel's matrices is presented in Figure 6. The result shows that the equilibrium state appeared after eight days of adsorption for all samples. The optimum drug loading appears in Chi-MA-22 samples with the highest methylene blue loading. Kinetic adsorption of methylene blue onto Chi-MA samples is determined using pseudo-first order and pseudo-second order kinetics (Aljeboree et al, 2017). The plot for both models is shown in Figure 6, while the parameter values are shown in Table 1. From the results, it can be concluded that pseudo-first order best fits all samples. Where q_t is the amount of methylene blue adsorbed at a given time (mg/g), and k_f is the first-order-adsorption kinetic constants (min^{-1}). The pseudo-first-order rate model primarily models the physical adsorption phenomenon, while the pseudo-second-order model primarily models the chemical adsorption phenomenon. According to the result, the kinetic has the best fit on the pseudo-first order model with higher R^2 compared to pseudo-second-order model. The physical adsorption occurred due to the interaction between positive charges of the methylene blue with the COO^- functional groups in the Chi-MA samples (Wirawan et al, 2022).

The equilibrium study is carried out by measuring the equilibrium concentration of methylene blue. The measurements are conducted at room temperature and several Chi-MA-22 doses involving two equilibrium models: Langmuir (Equation 5) and Freundlich (Equation 6), which are presented in Table 2. The Langmuir model consists of 2 parameters: full monolayer coverage (q_m) and Langmuir constant (k_L). While in the Freundlich model,

K_f and $1/n$ stand for adsorption capacity and adsorption intensity, respectively (Ayawei et al, 2017). Another study (Nadtoka et al., 2020) conducted methylene blue loading on hydrogels. They use a small increment time which resulting an adsorption equilibrium at about 140 min. This result might be because the monolayer adsorption has been reached. An extended time conducted in our study shows that methylene blue shows an equilibrium reached after about eight days which follows the Freundlich equilibrium model. This means that methylene blue is adsorbed at multilayer adsorption. In contrast, the Langmuir adsorption model assumes that the methylene blue is adsorbed at monolayer adsorption (Wirawan et al, 2022). In multilayer adsorption, the phenomena only occur in the physical adsorption mechanism, which is in line with the kinetics result.

Table 1 Kinetic Parameter Values of Each Model

Samples	Pseudo-First-Order			Pseudo-Second-Order		
	$k_f\ (day^{-1})$	$q_e(mg/g)$	R^2	$k_s\ (g/(mg\ day)$	$q_e(mg/g)$	R^2
Chi-MA-21	3.17×10^{-1}	13.25	0.9552	1.29×10^{-2}	18.8186	0.9444
Chi-MA-22	3.03×10^{-1}	19.92	0.9580	8.04×10^{-2}	28.5435	0.9487
Chi-MA-24	2.87×10^{-1}	15.79	0.9618	9.30×10^{-3}	22.9023	0.9534

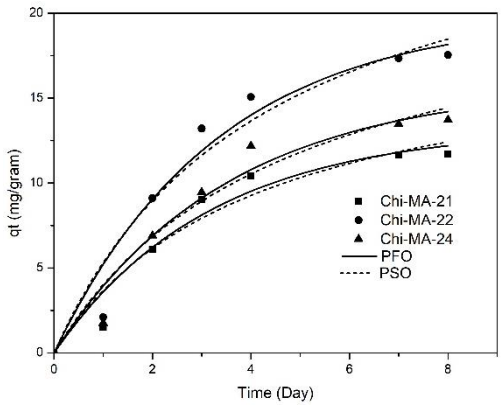

Figure 6 Methylene Blue Loading into Chi-MA Samples

Table 2 Adsorption Equilibrium Parameter Values of Each Model

Equilibrium Model	Parameters	Value
Langmuir	$q_m, mg/g$	570325
	$k_L, L/g$	4.09×10^{-5}
	R^2	0.8187
Freundlich	K_f	4.92
	$1/n$	2.19
	R^2	0.9640

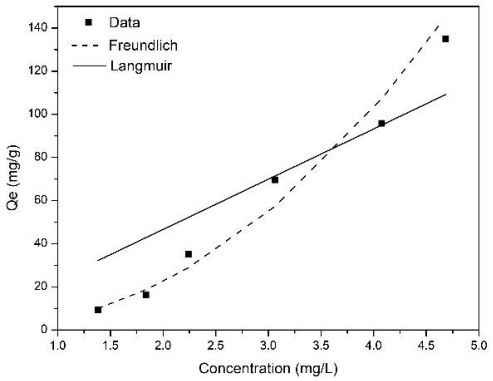

Figure 7 Adsorption Isotherm of Methylene Blue in Chi-MA-22

4. Conclusions

The chitosan-graft-maleic sponge was synthesized using the lyophilization method. The maximum ratio of maleic anhydride to chitosan mass ratio is 2:1. According to the result, the reaction and lyophilization were successfully conducted, which showed by the appearance of a peak at 1560.13 cm^{-1}, corresponding to the C=C bond. The shift in the peak rate of degradation in the second stage occurred at 300°C for pure chitosan and at 340°C for a graft-chitosan-maleate sponge. The methylene blue loading followed a pseudo-first-order kinetics model with k_f values varying from 0.287 – 0.317 day^{-1}. While the adsorption isotherm was best fitted with the Freundlich isotherm model with K_f and 1/n values are 4.92 and 2.19, respectively. Hence it can be concluded that a chitosan-graft-maleic sponge can be used as a methylene blue carrier.

Acknowledgments

The authors would like to acknowledge Ministry of Education and Culture of Indonesia for the financial support through PDUPT scheme (No. 2573/UN1-DITLIT/DIT-LIT/LT/2019) and partial support from SEAMEO for providing financial support under the University Consortium Seed Fund for Collaborative Research Grant. The authors also would like to extend their gratitude to the Universitas Gadjah Mada and Universiti Putra Malaysia for the research facilities and raw materials for completing this study.

References

Ali, A., Ahmed, S., 2018. A Review on Chitosan and Its Nanocomposites in Drug Delivery. *International Journal of Biological Macromolecules*, Volume 109, pp. 273–286

Aljeboree, A.M., Alshirifi, A.N., Alkaim, A.F., 2017. Kinetics and Equilibrium Study for the Adsorption of Textile Dyes on Coconut Shell Activated Carbon. *Arabian Journal of Chemistry*, Volume 10, pp. S3381–S3393

Ayawei, N., Ebelegi, A.N., Wankasi, D., 2017. Modeling and Interpretation of Adsorption Isotherms. *Journal Chemistry*, Volume 2017, p. 3039817

Ashley, E.A., Phyo. A.P., 2018. Drugs in Development for Malaria. *Drugs*, Volume 78(9), pp 861-879

Barleany, D.R., Ananta, C.V., Maulina, F., Rochmat, A., Alwan, H., Erizal, 2020. Controlled Release of Metformin Hydrogen Chloride from Stimuli-Responsive Hydrogel Based on Poly(N-Isoprpylacrylamide)/Chitosan/Polyvinyl Alcohol Composite. *International Journal of Technology*, Volume 11(3), pp. 511–521

Cai, B., Zhong, T., Chen, P., Fu, J., Jin, Y., Liu, Y., Huang, R., Tan, L., 2018. Preparation, Characterization and In Vitro Release Study of Drug-Loaded Sodium Carboxymethyl Cellulose/Chitosan Composite Sponge. *PLoS ONE*, Volume 13(10), pp. e0206275

Croisier, F., Jérôme, C., 2013. Chitosan-Based Biomaterials for Tissue Engineering. *European Polymer Journal*, Volume 49, pp. 780–792

Deb, P., Deoghare, A.B., Borah, A., Barua, E., Lala, S.D., 2018. Scaffold Development Using Biomaterials: A Review. *Materials Today: Proceedings*, Volume 5(5), pp. 12909–12919

Haerudin, H., Pramono, A.W., Kusuma, D.S., Jenie, A., Voelcker, N.H., Gibson, C., 2010. Preparation and Characterization of Chitosan/Montmorillonite (MMT) Nanocomposite Systems. *International Journal of Technology*, Volume 1(1), pp. 65–73

Hamedi, H., Moradi, S., Hudson, S.M., Tonelli, A.E., 2018. Chitosan Based Hydrogels and Their Application for Drug Delivery in Wound Dressing: A Review. *Carbohydrate Polymers*, Volume 199, pp. 445–460

Horio, T., Isihara, M., Fujita, M., Kishimoto, S., Kanatani, Y., Ishizuka, T., Nogami, Y., Nakamura, S., Tanaka, Y., Morimoto, Y., Maehara, T., 2010. Effect of Photocrosslinkable Chitosan Hydrogel and Its Sponges to Stop Bleeding in a Rat Liver Injury Model, *Artificial Organs*, Volume 34(4), pp. 342–347

Kassem, M.A.A., Elmeshad, A.N., Fares, A.R., 2015. Lyophilized Sustained Release Mucoadhesive Chitosan Sponges for Buccal Buspirone Hydrochloride Delivery: Formulation and *In Vitro* Evaluation. *AAPS PharmSciTech*, Volume 16(3), pp. 537–547

Knidri, H.E., Belaabed, R., Addaou, A., Laajeb, A., Lahsini, A., 2018. Extraction, Chemical Modification, and Characterization of Chitin and Chitosan. *International Journal of Biological Macromolecules*, Volume 120, pp. 1181–1189

Kono, H., Oeda, I., Nakamura, T., 2013. The Preparation, Swelling Characteristics, and Albumin Adsorption and Release Behaviors of a Novel Chitosan-Based Polyampholyte Hydrogel. *Reactive & Functional Polymers*, Volume 73, pp. 97–107

Krisanti, E.A., Lazuardi, D., Kiresya, K.K., Mulia, K., 2020. Tablet Formulation Containing Chitosan-Alginate Microparticles: Characterization and Release Profile of Xanthones. *International Journal of Technology*, Volume 11(5), pp. 900–909

Kumar, S., Koh, J., 2012. Physiochemical, Optical and Biological Activity of Chitosan-Chromone Derivative for Biomedical Applications. *International Journal of Molecular Sciences*, Volume 13, pp. 6102–6116

Kusumastuti, Y., Shibasaki, Y., Hirohara, S., Kobayashi, M., Terada, K., Ando, T., Tanihara, M., 2017. Encapsulation of Rat Bone Marrow Stromal Cells using a Poly-Ion Complex Gel of Chitosan and Succinylated Poly (Pro-Hyp-Gly). *Journal of Tissue Engineering and Regenerative Medicine*, Volume 11(3), pp. 869–876

Kusumastuti, Y., Timotius, D., Putri, N.R.E., Syabani, M.W., Rochmadi, 2020. Rheological and Kinetic Studies of Low-Density Polyethylene (LDPE)-Chitosan Biocomposite Film. *IOP Conference Series: Materials Science and Engineering*, Volume 722, p. 012054

Lavanya, R., Gomathi, T., Vijayalakshmi, K., Saranya, M., Sudha, P.N., 2017. Adsorptive Removal of Copper (II) and Lead (II) Using Chitosan-g-Maleic Anhydride-g-Methacrylic Acid Copolymer. *International Journal of Biological Macromolecules*, Volume 104, pp. 1495–1508

Liu, R., Xu, X., Zhuang, X., Cheng, B., 2014. Solution Blowing of Chitosan/PVA Hydrogels Nanofiber Mats. *Carbohydrate Polymers*, Volume 101, pp. 1116–1121

Liu, Y., Shen, X., Zhou, H., Wang, Y., Deng, L., 2016. Chemical Modification of Chitosan Film Via Surface Grafting of Citric Acid Molecular to Promote Biomineralization. *Applied Surface Science*, Volume 370, pp. 270–278

Nadtoka, O., Virych, P., Kutsevol, N., 2020. Hydrogels Loaded with Methylene Blue: Sorption-Desorption and Antimicrobial Photoactivation Study. *International Journal of Polymer Science*, Volume 2020, p. 9875290

Nikolova, M.P., Chavali, M.S., 2019. Recent Advances in Biomaterials for 3D Scaffolds: A Review. *Bioactive Materials*, Volume 4, pp. 271–292

Patel, S., Srivastava, S., Singh, M.R., Singh, D., 2018. Preparation and Optimization of Chitosan-Gelatin Films for Sustained Delivery of Lupeol for Wound Healing. *International journal of Biological Macromolecules*, Volume 107(Part B), pp. 1888–1897

Peers, S., Montembault, A., Ladavière, C., 2020. Chitosan Hydrogels for Sustained Drug Delivery. *Journal of Controlled Release*, Volume 326, pp. 150–163

Pottathara, Y.B., Vuhere, T., Maver, U., Kokol, V., 2021. Morphological, Mechanical, and In-Vitro Bioactivity of Gelatine/Collagen/Hydroxyapatite Based Scaffolds Prepared by Unidirectional Freeze-Casting. *Polymer Testing*. Volume 102, p. 107308

Schirmer, R.H., Adler, H., Pickhardt., Mandelkow, E., 2011. Lest We Forget You – Methylene Blue. *Neurobiology of Aging*, Volume 32(12), pp. e7–e16

Sinha, V.R., Singla, S.K., Wardhawan, S., Kaushik, R., Kumria, R., Bansal, K., Dhawan, S., 2004. Chitosan Microspheres as a Potential Carrier for Drugs. *International Journal of Pharmaceutics*, Volume 274, pp. 1–33

Syafiuddin, A., Salmiati, S., Jonbi, J., Fulazzaky, M.A., 2018. Application of the Kinetic and Isotherm Models for Better for Better Understanding of the Behaviors of Silver Nanoparticles Adsorption onto Different Adsorbents. *Journal of Environmental Management*, Volume 218, pp. 59–70

Timotius, D., Kusumastuti, Y., Rochmadi., 2022. Characterization and Equilibrium Study of Drug Release of pH-Responsive Chitosan-graft-Maleic Film. *International Journal of Technology*, Volume 13(2), pp. 398–409

Wirawan, S.K., Timotius, D., Nugraha, I.M., Restana, A., Anggara, A.L., Hidayatullah, S., 2022. Kinetics and Adsorption Equilibrium Study of Free Fatty Acid (FFA) from Crude Palm Oil (CPO) on Anionic Resin. *ASEAN Journal of Chemical Engineering*, Volume 22(1), pp. 33–41

Xue, H., Thaivalappil, A., Cao, K., 2021. The Potentials of Methylene Blue as an Anti-Aging Drug. *Cells*. Volume 10(12), p. 3379

Zhou, Y., Dong, Q., Yang, H., Liu, X., Yin, X., Tao Y., Bai, Z., Xu, W., 2017. Photocrosslinked Maleilated Chitosan/Methacrylated Poly (Vinyl Alcohol) Bicomponent Nanofibrous Scaffolds for Use as Potential Wound Dressings. *Carbohydrate Polymers*, Volume 168, pp. 220–226